LBL-36005
UC-413

Lawrence Berkeley Laboratory
UNIVERSITY OF CALIFORNIA

Presented at the Fourth KINR International School on Nuclear Physics, Kiev, Ukraine, August 29–September 7, 1994, and to be published in the Proceedings

Thomas-Fermi Treatment of Nuclear Masses, Deformations and Density Distributions

W.D. Myers and W.J. Świątecki

August 1994

REFERENCE COPY
Does Not
Circulate
Bldg. 50 Library.
Copy 1
LBL-36005

Prepared for the U.S. Department of Energy under Contract Number DE-AC03-76SF00098

DISCLAIMER

This document was prepared as an account of work sponsored by the United States Government. While this document is believed to contain correct information, neither the United States Government nor any agency thereof, nor the Regents of the University of California, nor any of their employees, makes any warranty, express or implied, or assumes any legal responsibility for the accuracy, completeness, or usefulness of any information, apparatus, product, or process disclosed, or represents that its use would not infringe privately owned rights. Reference herein to any specific commercial product, process, or service by its trade name, trademark, manufacturer, or otherwise, does not necessarily constitute or imply its endorsement, recommendation, or favoring by the United States Government or any agency thereof, or the Regents of the University of California. The views and opinions of authors expressed herein do not necessarily state or reflect those of the United States Government or any agency thereof or the Regents of the University of California.

LBL-36005
UC-413

Thomas-Fermi Treatment of Nuclear Masses, Deformations and Density Distributions

W.D. Myers and W.J. Świątecki

Nuclear Science Division
Lawrence Berkeley Laboratory
University of California
Berkeley, California 94720

August 1994

This work was supported by the Director, Office of Energy Research, Office of High Energy and Nuclear Physics, Division of Nuclear Physics, and by the Office of Basic Energy Sciences, Division of Nuclear Sciences, of the U.S. Department of Energy under Contract No. DE-AC03-76SF00098.

THOMAS-FERMI TREATMENT OF NUCLEAR MASSES, DEFORMATIONS AND DENSITY DISTRIBUTIONS*

LBL-36005

W.D. Myers and W.J. Świątecki

Nuclear Science Division
Lawrence Berkeley Laboratory
1 Cyclotron Road
Berkeley, California 94720
USA

Abstract

A recently completed Thomas-Fermi model of nuclei is described. Six adjustable parameters of the effective nucleon-nucleon interaction were fitted to the shell-corrected binding energies of 1654 nuclei and to the diffuseness of the nuclear surface. The model is then successful in reproducing nuclear sizes, and only small deviations are found between calculated and measured fission barriers of 36 nuclei. The model is applied to the prediction of fission barriers of light elements, to drip-line nuclei like ^{82}Sn and ^{170}Sn, to the properties of nuclear and neutron matter and to nuclear bubble configurations with $Z^2/A \approx 100$. The relation of a Thomas-Fermi theory to the Droplet and Liquid Drop models is illustrated.

1. INTRODUCTION

It is a great pleasure to take part in this conference honoring Vilen Strutinsky, and to visit Kiev, the ancient capital of the Ukraine.

Strutinsky's shell correction method, developed in the sixties, considers the nuclear binding energy to be made up of a microscopic contribution added to a smooth macroscopic background. The success of Strutinsky's treatment of the microscopic part revolutionized overnight the calculation of nuclear binding and deformation energies. Less dramatic and more gradual advances have also been made in the macroscopic background energy. In the early calculations the macroscopic part was usually a simple liquid drop formula. Later, a Droplet Model was often used. A more nearly ideal smooth background is provided by a Thomas-Fermi model. My talk today will proceed in the reverse order. I will first describe a Thomas-Fermi model that Bill Myers and I have completed recently. Then I will illustrate how the Droplet Model (and the liquid Drop Model) are algebraic approximations to the Thomas-Fermi model.

*Talk presented by W.J. Świątecki at the fourth KINR International School on Nuclear Physics, Kiev, August 29–September 7, 1994.

2. THE THOMAS-FERMI MODEL

This model is based on the beautiful statistical method introduced into atomic physics by L.H. Thomas [1] and, independently, by E. Fermi [2] in 1926–27. It says that for a degenerate gas of fermions the density of particles in phase space is 2 per h^3. From this one can deduce at once any shell-averaged semi-classical property of electrons in atoms and molecules [3]. The scheme gives results that are essentially equivalent to a Hartree or Hartree-Fock calculation averaged over shell effects.

Our own starting point was the straightforward Thomas-Fermi treatment of nuclei introduced by Seyler and Blanchard in their papers from 1961 and 1963 [4]. Thus we have *no* density-gradient corrections or higher-order terms in an expansion in $\hbar$ [5–13] — just the pure Thomas-Fermi model. We have, however, generalized the Seyler-Blanchard effective nucleon-nucleon Yukawa interaction v_{12} by adding one momentum-dependent and one density-dependent term [14]:

$$v_{12} = 2T_0\rho_0^{-1}\cdot Y(r_{12})\cdot\Big[\underbrace{-\alpha+\beta(p_{12}/P_0)^2-\gamma(p_{12}/P_0)^{-1}}_{\text{Seyler–Blanchard}}+\sigma(2\bar{\rho}/\rho_0)^{2/3}\Big] \tag{1}$$

Extra attraction increases when p_{12} is small (and particles would like to become correlated), and tends to zero for large p_{12}, when particles would zip past each other.

Repulsion increases with increasing average density $\bar{\rho}$.

Here T_0, P_0, ρ_0 are the Fermi energy, the Fermi momentum and the particle density of standard nuclear matter — these quantities serve as convenient units. $Y(r_{12})$ is a Yukawa interaction of range a:

$$Y(r_{12}) = \frac{1}{4\pi a^3}\frac{e^{-r_{12}/a}}{r_{12}/a} \quad . \tag{2}$$

The distance between the particles is r_{12} and p_{12} is the magnitude of their relative momentum. The average density $\bar{\rho}$ is defined by

$$\bar{\rho}^{2/3} = \left(\rho_1^{2/3}+\rho_2^{2/3}\right)/2 \quad , \tag{3}$$

where ρ_1 and ρ_2 are the densities of the interacting particles at points 1 and 2. The dimensionless interaction strength parameters $\alpha, \beta, \gamma, \sigma$ may be different for interactions between like particles (neutron-neutron, proton-proton) and unlike particles (neutron-proton). The difference is described in our model with the aid of two parameters ξ and ζ as follows:

$$\alpha_\ell = \frac{1}{2}(1-\xi)\alpha \quad , \qquad \alpha_u = \frac{1}{2}(1+\xi)\alpha \quad ,$$

$$\left.\begin{matrix}\beta_\ell \\ \gamma_\ell \\ \sigma_\ell\end{matrix}\right\} = \frac{1}{2}(1-\zeta)\left\{\begin{matrix}\beta \\ \gamma \\ \sigma\end{matrix}\right. , \qquad \left.\begin{matrix}\beta_u \\ \gamma_u \\ \sigma_u\end{matrix}\right\} = \frac{1}{2}(1+\zeta)\left\{\begin{matrix}\beta \\ \gamma \\ \sigma\end{matrix}\right. . \tag{4}$$

Altogether there are seven adjustable parameters in our model: α, β, γ, σ, ξ, ζ and the range a. It turns out that nuclear energies and density distributions depend on only *six* parameters, because for them β and σ always occur together in the combination $B \equiv \beta + (5/6)\,\sigma$ [14]. (This degeneracy is broken if the Thomas-Fermi model is used to calculate the depth of the optical model potential, but I will leave this aspect out in the present talk.)

3. FITTING THE PARAMETERS

The description of the techniques used to solve the self-consistent nuclear Thomas-Fermi equations may be found in [14] and [15]. Suffice it to say that we have now available fast and robust iterative schemes that give accurate solutions of the Thomas-Fermi equations for shapes with or without spherical symmetry.

We used these methods to calculate, for a given set of the 6 adjustable parameters, the binding energies of 1654 nuclei according to the expression

$$E = \text{T.F.} + \text{Shells} + \text{Odd-even} + W \quad . \tag{5}$$

Here T.F. is the result of the Thomas-Fermi calculation, "Shells" is the Strutinsky shell correction taken from [16] (column headed E_{mic}), the odd-even correction is ± 11 MeV/$\sqrt{A}$ for odd or even nuclei and zero for odd-mass nuclei, and W is the Wigner term from [17]: $W = -7$ MeV $\exp(-6|I|)$, where $I = (N-Z)/A$. We also solved the Thomas-Fermi equations for semi-infinite standard nuclear matter and determined the Süssmann width b_0 (diffuseness) [18] of the nuclear surface for the given set of parameters. (The value $b_0 = 1.0$ fm gives reasonable agreement with measurements of nuclear charge distributions.) We then minimized the RMS deviation of the calculated from the measured binding energies of the 1654 nuclei by a search in the five-dimensional parameter sub-space for which b_0 remains equal to 1 fm. This led to a minimum RMS equal to 0.711 MeV and to the following set of parameters: $\alpha = 1.98483$, $B = 1.03290$, $\gamma = 1.10121$, $\xi = 0.25771$, $\zeta = 0.53002$ and $a = 0.59346$ fm. (An analysis of optical model potentials provides further the value $\sigma = 1.05$, and hence gives $\beta = 0.15790$, [19].)

4. SOME CONSEQUENCES

a) Nuclear Matter

The following properties of nuclear matter follow from the above set of parameters:

- Four Liquid Drop Properties

Radius constant of standard nuclear matter	$r_0 = 1.14$ fm
Volume binding coefficient	$a_1 = 16.04$ MeV
Symmetry energy coefficient	$J = 32$ MeV
Surface energy coefficient	$a_2 = 18.5$ MeV

- Five Droplet Model Properties [20]

Compressibility coefficient	$K = 234$ MeV
Curvature energy coefficient	$a_3 = 12$ MeV
Effective surface stiffness coefficient	$Q = 34$ MeV
Density-symmetry coefficient	$L = 50$ MeV
Symmetry-anharmonicity coefficient	$M = 7$ MeV

b) Neutron Matter

Figure 1 shows the energy per particle of neutron matter at density ρ_n as a function of the density parameter $\Phi \equiv (\rho_n/\frac{1}{2}\rho_0)^{1/3}$. There is a striking correspondence with the theoretical estimate of [21], which is based on entirely different physical input.

c) Nuclear Charge Distributions

Figure 2 shows the calculated charge distributions for ^{56}Fe, ^{124}Sn and ^{209}Bi compared with Woods-Saxon or three-parameter Gaussian fits to measurements [22]. The radius constant $r_0 = 1.14$ fm, deduced from a fit to masses, is just about perfect in reproducing measured nuclear sizes.

d) Fission Barriers

Figure 3 shows calculated fission barriers down to very light nuclei (diamonds) and a comparison with 36 measured barriers (corrected for ground state shell effects) for nuclei with $71 \leq Z \leq 98$ (black squares). The triangles show the discrepancies, which become noticeable below $Z \approx 84$.

e) Drip-line Nuclei

Figure 4 shows the chemical potentials for isotopes of Sn from neutron number $N = 120$ down to $N = 32$. These numbers define the neutron drip line and the classical proton drip line (i.e., the drip line in the absence of quantal barrier penetration) in the Thomas-Fermi model without shell and

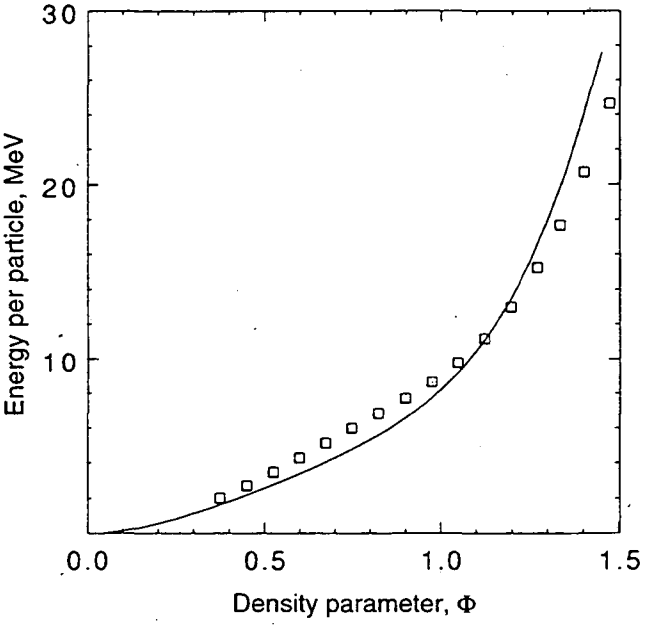

Figure 1. The energy per particle of neutron matter according to [21] (squares), compared with our Thomas-Fermi result [19].

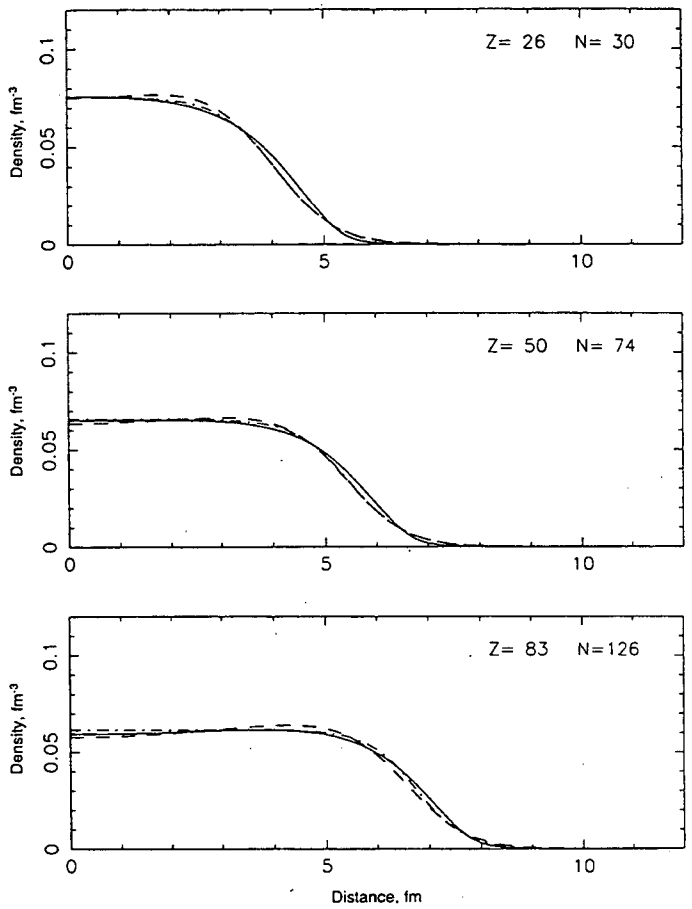

Figure 2. The Thomas-Fermi charge distributions for three nuclei [19] are compared with Woods-Saxon (dot-dashed) or three-parameter Gaussian (dashed) fits to measurements [22].

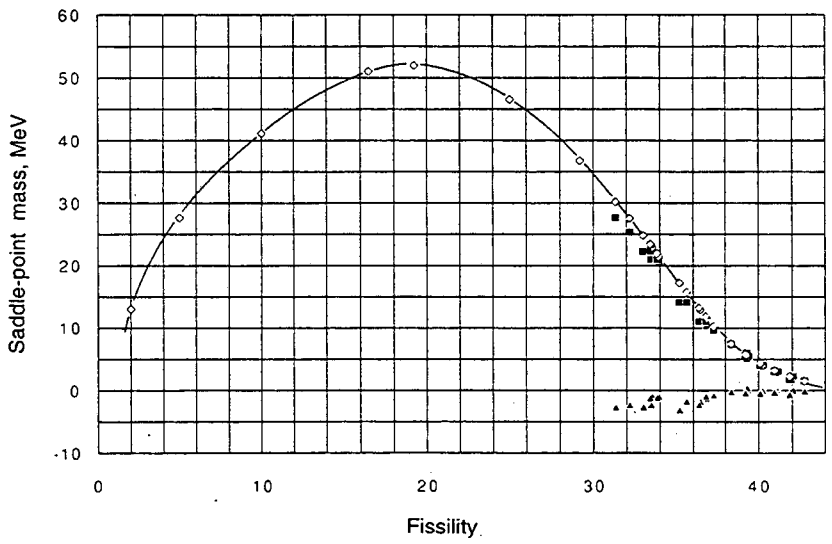

Figure 3. Calculated [19] fission barriers (diamonds) are compared with 36 measured barriers corrected for ground-state shell effects. The triangles show the difference. (Here a parameter set based on $r_0 = 1.145$ fm was used. With the canonical set quoted in the text, the calculated barriers would be higher by less than 0.5 MeV.) The "fissility," defined as $Z^2/A(1-2.2I^2)$, makes the calculated points conform closely to a single curve.

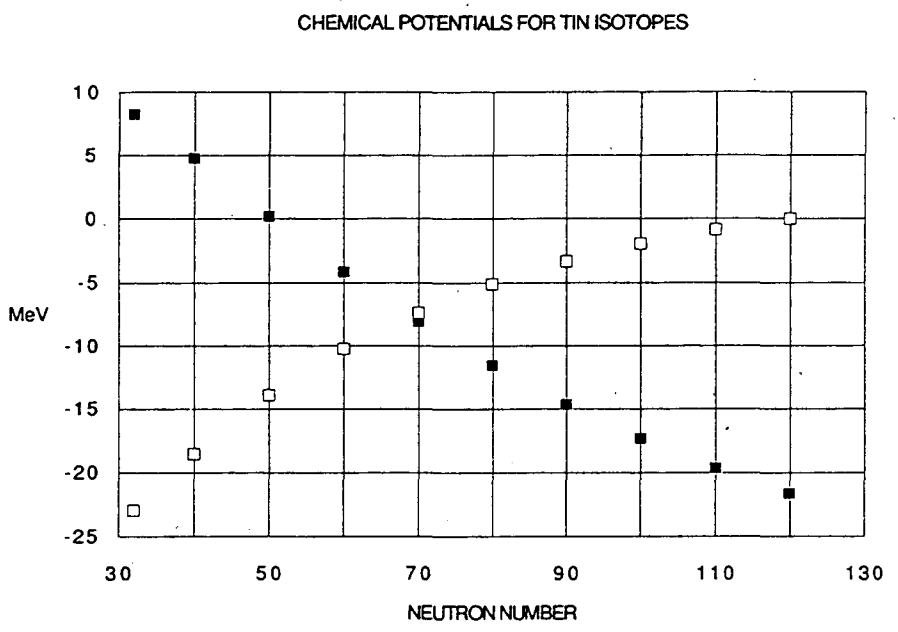

Figure 4. The Thomas-Fermi chemical potentials (separation energies) for Sn isotopes vs neutron number [19].

pairing effects. Figure 5 illustrates the density distributions for ^{120}Sn and for the two exotic drip line isotopes ^{82}Sn and ^{170}Sn.

f) A Nuclear Bubble [23,24]

Figure 6 shows the last unruptured nucleus ($N = 372$, $Z = 248$, $Z^2/A = 99.2$) and the first bubble nucleus ($N = 378$, $Z = 252$, $Z^2/A = 100.8$) in a sequence of increasingly heavier nuclei (constrained to spherical symmetry) for which $(N-Z)/A = 0.2$.

In summary, we now have a workable statistical model of nuclei that can be used in a variety of applications. In addition to combining it with Strutinsky shell corrections in order to give a good account of nuclear binding energies, it can be subjected to various extreme conditions. Some of them I already indicated. In the future we will be investigating the effects of large angular momenta on the ground-state and saddle-point properties of these shell-averaged idealized nuclei.

5. THE DROPLET MODEL

The Droplet Model [20,25] is defined in terms of an expansion in powers of $A^{-1/3}$ and I^2 that claims to reproduce quantitatively the principal features of *any* self-consistent, shell-averaged nuclear calculation, provided that $A^{-1/3}$ and I^2 are sufficiently small. The claim is that, given the nine parameters listed in Section 4(a) — which are properties of infinite or semi-infinite nuclear matter — one can then predict the energies and density distributions of *finite* nuclei in terms of closed algebraic expressions, accurate to relative order $(A^{-1/3})^2$ and I^4. Here are a couple of examples to show how it works.

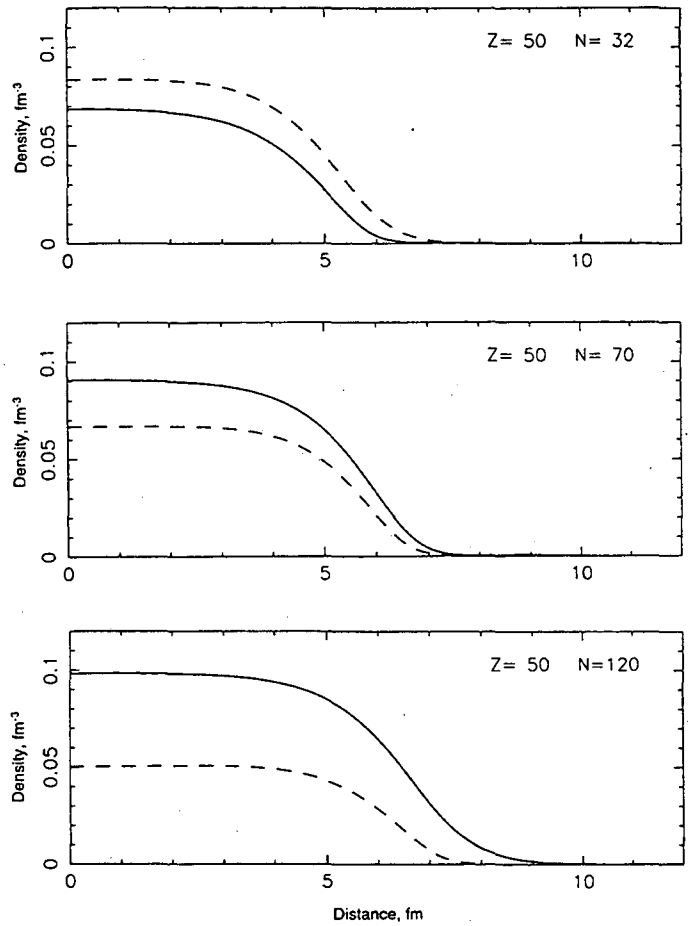

Figure 5. The neutron (solid) and proton (dashed) density distributions for Sn isotopes [19].

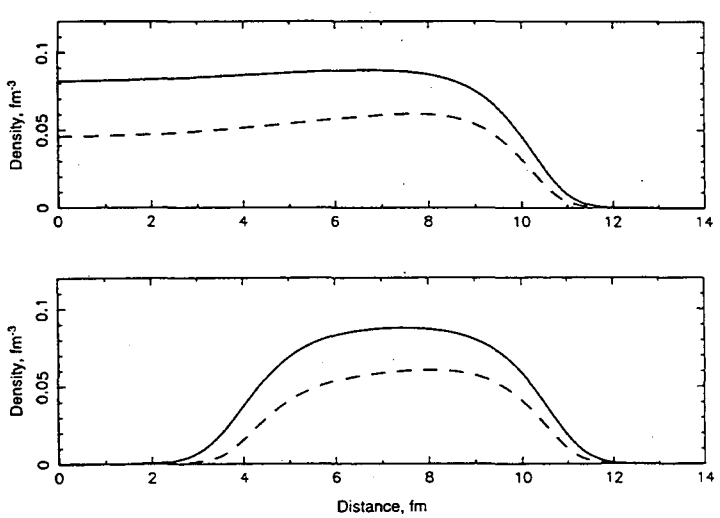

Figure 6. The last unruptured (A = 620) and the first bubble (A = 630) nucleus in a sequence where A is increased while (N-Z)/A is kept fixed at 0.2 [19].

(a) Binding Energies

The Droplet Model formula for the energy of a nucleus with N = Z and the Coulomb energy switched off is

$$E = -a_1 A + a_2 A^{2/3} + \left(a_3 - \frac{2a_2^2}{K} \right) A^{1/3} \quad , \tag{6}$$

or

$$E = -15.677A + 18.56A^{2/3} + 7.00A^{1/3} \quad \text{MeV} \quad , \tag{7}$$

if, for illustrative purposes, one takes the parameters from our 1969 Thomas Fermi model [25]. The actual Thomas-Fermi calculations deviate from the first two terms by an amount that can be represented by 6.98 $A^{-1/3}$ MeV (plus higher order terms), thus confirming the Droplet Model prediction (see Fig. 25 in [25]). Figure 7 shows E/A plotted vs $A^{-1/3}$.

The Droplet Model predicts further that when $N \neq Z$ the additional symmetry energy can be written as

$$\Delta E = J_{eff} A I^2 \quad , \tag{8}$$

where $J_{eff} = J/(1 + \omega A^{-1/3})$ and $\omega = \frac{9}{4}\frac{J}{Q} - \frac{2a_2 L}{KJ}$. Figure 8 compares this prediction with Thomas-Fermi calculations from [25].

(b) Densities

The Droplet Model predicts the form of an equivalent sharp-surfaced "generating density," which can be used to generate an approximation to the actual diffuse density by convoluting it with a suitable short-range function. *Away* from the surface the generating density itself should agree with a Thomas-Fermi calculation. Figure 9 compares the neutron and proton

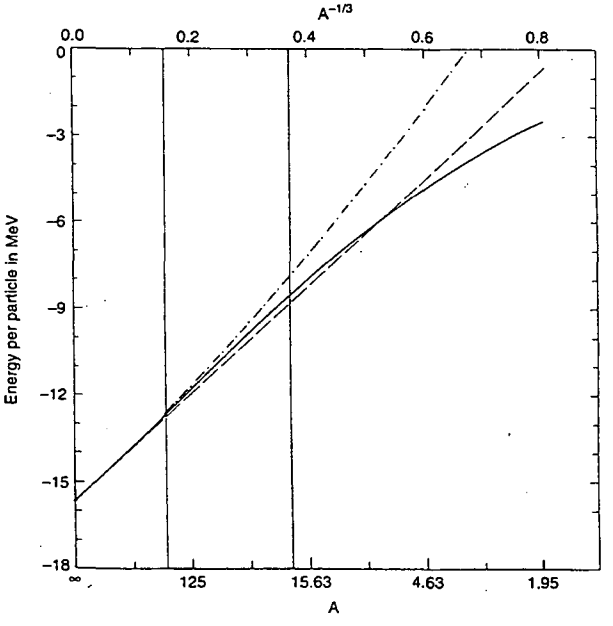

Figure 7. A Thomas-Fermi binding energy per particle is plotted vs $A^{-1/3}$ (solid curve) and the result is compared with the liquid drop approximation (dashed line) and the Droplet Model formula, eq. (7) (dot-dashed). A detailed comparison shows that the Droplet Model gives a perfect representation of the Thomas-Fermi curve for small $A^{-1/3}$, but in the region of actual nuclei (between the two vertical lines) higher-order terms conspire to give to the Thomas-Fermi curve a linear appearance, suggesting erroneously the absence of a curvature energy. (Parameters from [25].)

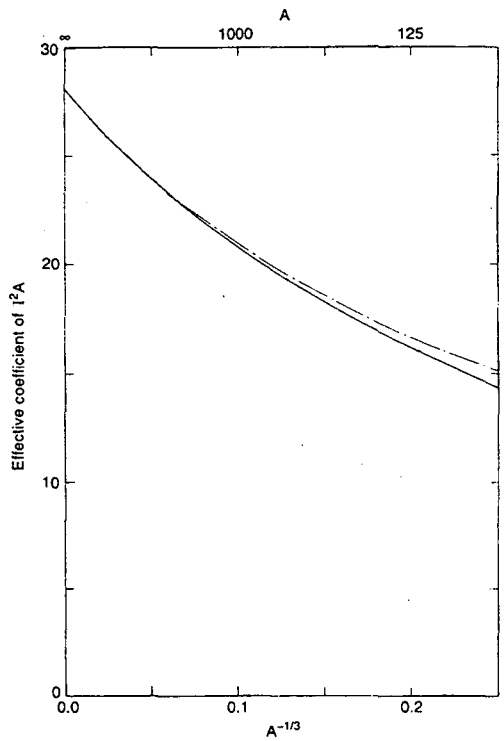

Figure 8. The effective Droplet Model symmetry energy J_{eff} from eq. (8) (dot-dashed) is compared with a Thomas-Fermi calculation. (Parameters from [25].)

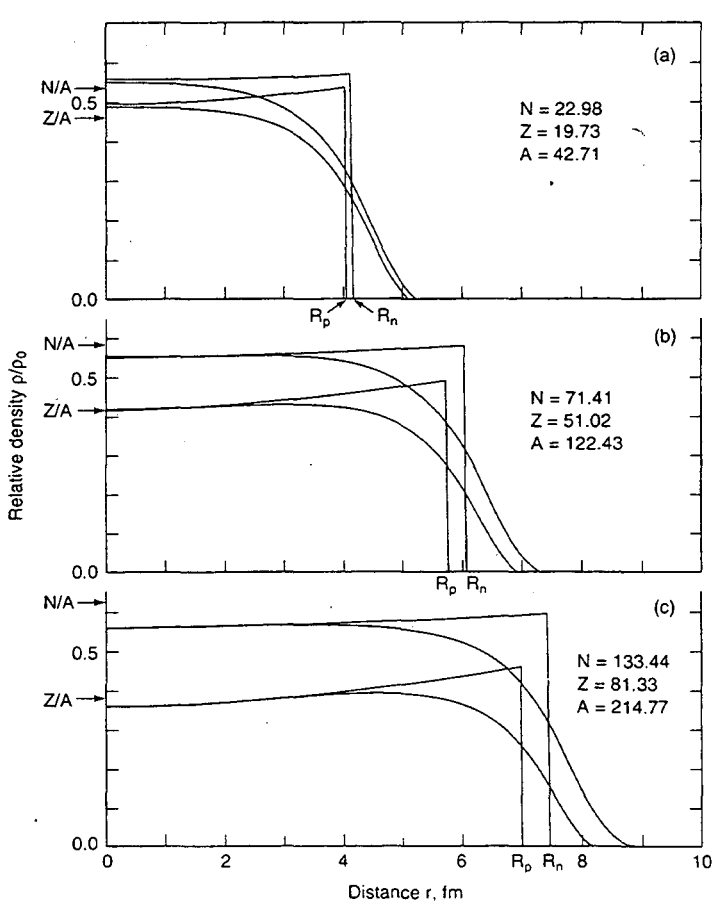

Figure 9. The Droplet Model neutron and proton densities from eq. (9) are compared with Thomas-Fermi (point) densities. (Parameters from [25].)

densities for three Thomas-Fermi nuclei, taken from [25], with the corresponding Droplet Model generating densities. In the bulk the agreement is virtually perfect down to $A \approx 43$.

[The Droplet Model expressions for the neutron and proton densities are as follows

$$\rho_n = \bar{\rho}_n + \tilde{\rho}_n \quad , \quad \rho_p = \bar{\rho}_p + \tilde{\rho}_p \tag{9}$$

$$\bar{\rho}_n / \rho_o = \tfrac{1}{2}(1 - 3\bar{\varepsilon} + \bar{\delta}) \quad , \quad \bar{\rho}_p / \rho_o = \tfrac{1}{2}(1 - 3\bar{\varepsilon} - \bar{\delta}) \tag{10}$$

$$\tilde{\rho}_n / \rho_o = \tfrac{1}{2}(-3\tilde{\varepsilon} + \tilde{\delta}) \quad , \quad \tilde{\rho}_p / \rho_o = \tfrac{1}{2}(-3\tilde{\varepsilon} - \tilde{\delta}) \tag{11}$$

$$\bar{\delta} = \left(1 + \frac{3}{8}\frac{c_1}{Q}\frac{Z^2}{A^{5/3}}\right) \Big/ \left(1 + \frac{9}{4}\frac{J}{Q}A^{-1/3}\right) \tag{12}$$

$$\bar{\varepsilon} = (-2a_2 A^{-1/3} + L\bar{\delta}^2 + c_1 Z^2 / A^{4/3}) / K \tag{13}$$

$$\tilde{\delta} = (Ze^2 / 4JR_0) \Big/ \left[\tfrac{3}{10} - \tfrac{1}{2}(r / R_0)^2\right] \tag{14}$$

$$\tilde{\varepsilon} = (6J / K)\,\tilde{\delta} \tag{15}$$

$$R_0 = r_0 A^{1/3} \quad , \quad \rho_0 = 1 / \left(\tfrac{4}{3}\pi r_0^3\right) \quad , \quad c_1 = 3e^2 / 5r_0 \tag{16}$$

$$R_n / R_0 = (N\rho_0 / A\bar{\rho}_n)^{1/3} \quad R_p / R_0 = (Z\rho_0 / A\bar{\rho}_p)^{1/3} \quad , \tag{17}$$

where e is the charge unit, and the values of the Droplet Model parameters r_0, a_1, a_2, J, K, Q, L used to construct Fig. 9 were taken from [25].]

A characteristic feature of the Droplet Model, seen in Fig. 9, is that the generating densities for neutrons and protons have different equivalent sharp radii, and that the bulk densities become slightly non-uniform under the influence of the Coulomb repulsion. If these two effects are suppressed, there results the Liquid Drop Model, with a single equivalent sharp surface and uniform bulk densities.

This, roughly speaking, is the relation between the Thomas-Fermi, the Droplet and the Liquid Drop Models. Which one to use in practice? Each has its advantages and disadvantages. Nothing can beat the simplicity of the Liquid Drop Model. At the other extreme, the Thomas-Fermi model is close to an ideal macroscopic description, without the limitations of the Droplet Model, which fails when $A^{-1/3}$ or I^2 are too large. But the Droplet Model has the advantage of being an algebraic scheme, and there are situations where it is the model of choice, as illustrated by the theory of the electric dipole moments of deformed nuclei.

(c) Dipole Moments

The Droplet Model provides a formula [27,28] for the macroscopic contribution to the electric dipole moment d (in units of the proton charge) of a deformed nucleus, whose surface is described in terms of Legendre Polynomials $P_\ell(\cos\theta)$:

$$R(\theta) = R_0\left(1+\sum_2^\infty \alpha_\ell P_\ell(\cos\theta)\right) \quad . \tag{18}$$

Thus

$$\begin{aligned} d = {} & C_r \sum_{\ell=2}^{\infty} \frac{12(\ell-1)(\ell+1)(8\ell+9)}{5(2\ell+1)^2(2\ell+3)^2}\alpha_\ell\alpha_{\ell+1} \\ & -C_s \sum_{\ell=2}^{\infty} \frac{(\ell-1)(\ell+1)(\ell+3)}{(2\ell+1)(2\ell+3)}\alpha_\ell\alpha_{\ell+1} \\ & + \text{terms of higher order in the } \alpha_\ell\text{'s} \quad , \end{aligned} \tag{19}$$

where

$$C_r = \frac{AZe^2}{8}\left[\frac{1}{J}+\frac{6L}{JK}I+\frac{15}{8Q}A^{-1/3}\right] \quad , \tag{20}$$

$$C_s = (2NZ/A)(I-\bar{\delta})R_0 \quad , \tag{21}$$

with $\bar{\delta}$, R_0 given by eqs. (12,16). It would be a thankless task to try to extract an amount of information comparable to that encapsulated in eq. (19) by performing dozens (thousands ?) of variously constrained Thomas-Fermi calculations.

6. THE CURVATURE ENERGY PUZZLE

As discussed in [29,30] there seems to be a difficulty in reconciling theoretical estimates of the curvature energy coefficient, which invariably give a_3 somewhere around 10 MeV, with empirical fits to binding energies and fission barriers, which are said to require $a_3 \approx 0$. Our Thomas-Fermi model does not seem to suffer from this conundrum: it is characterized by $a_3 = 12$ MeV, yet gives an acceptable fit to binding energies and barriers. To throw further light on this problem I made the following numerical experiment. With our current parameters, eq. (6) gives for the binding energy for uncharged N = Z nuclei the expression

$$E(A) = -16.04A + 18.5A^{2/3} + 9.1A^{1/3} - 11.56\ \text{MeV} \quad , \tag{22}$$

where I added the last term to represent missing higher-order terms which, in practice, make E tend to zero when A is small. I chose the value 11.56 to make E(A) vanish at A = 1. In a plot of the type of Fig. 7, this higher order term reverses the peeling off from the dashed straight line caused by the term proportional to $A^{1/3}$ in eq. (6). Now I fitted to eq. (22), *in the interval of nuclei from A ≈ 20 to A ≈ 260*, an expression $\bar{E}$ *without* the last two terms, i.e.,

$$\overline{E}(A) = -\overline{a}_1 A + \overline{a}_2 A^{2/3} \quad . \tag{23}$$

The least squares fit gave $\overline{a}_1 = 16.2119$ MeV, $\overline{a}_2 = 20.7265$ MeV, and the RMS deviation was — surprise — a mere quarter of an MeV out of binding energies ranging from 300 to 3000 MeV! In other words, because of the interplay between the $A^{1/3}$-term and the higher order terms, the plot of the binding energy per particle vs $A^{-1/3}$ *in the range of actual nuclei (except the lightest)* can be very nearly a straight line. This might lead one to the erroneous conclusion that there is no curvature correction when, in fact, a_3 is of the theoretically expected magnitude. My own feeling at the moment is that theoretical estimates of a_3 [30], including our Thomas-Fermi determination of a_3 as equal to 12 MeV, are probably not too far off. [If the energy per particle is written as

$$y = -a_1 + a_2 x + c_3 x^2 - c_4 x^3 \quad , \quad \text{where} \quad x \equiv A^{-1/3} \quad , \tag{24}$$

a straight-line approximation to y(x) in the interval $x_1 = 250^{-1/3} = 0.159$ to $x_2 = 20^{-1/3} = 0.368$ will be relatively accurate if the inflection point in y(x) falls not too far from the center of the interval, at $x = 0.264$.
With $c_3 = 9.1$, $c_4 = 11.56$, the inflection point is at $x = c_3/3c_4 = 0.262$.]

7. CONCLUSIONS

In describing theoretically the macroscopic part of nuclear energies we have available several approaches, ranging from the Liquid Drop Model, through the Droplet Model, to the Thomas-Fermi Model. The first two may, in fact, be regarded as leading approximations to the Thomas-Fermi theory in an expansion in $A^{-1/3}$ and I^2, as depicted in Fig. 10.

It would have been a pleasure to have discussed these refinements of the microscopic-macroscopic method with Vilen Strutinsky, who contributed so much to both aspects of this approach.

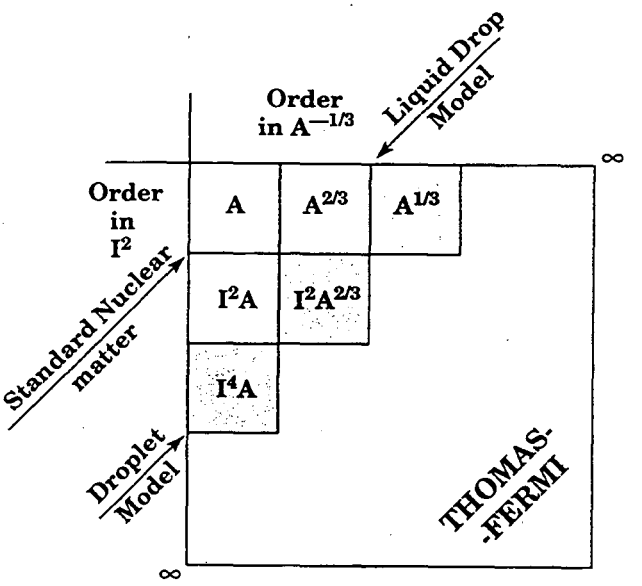

Figure 10. The description of a nucleus in the standard nuclear matter approximation and in the liquid drop and the Droplet Model formalisms may be considered as systematic approximations, based on expansions in $A^{-1/3}$ and I^2, to a Thomas-Fermi calculation.

ACKNOWLEDGEMENTS

We would like to thank P. Möller, J.R. Nix and Jan Černohorsky for help with data-handling and computer-related problems. This work was supported by the Director, Office of Energy Research, Office of High Energy and Nuclear Physics, Division of Nuclear Physics, and by the Office of Basic Energy Sciences, Division of Nuclear Sciences, of the U.S. Department of Energy under Contract No. DE-AC03-76SF00098.

REFERENCES

[1] L. H. Thomas, Proc. Cambridge Phil. Soc. **33**, 542 (1927).

[2] E. Fermi, Rend. Lincei **6**, 602 (1927); Zeit. f. Physik **48**, 73 (1928).

[3] P. Gombas, "Die statistische Theorie des Atoms und ihre Anwendung" (Springer, Wien, 1949).

[4] R. G. Seyler and C. H. Blanchard, Phys. Rev. **124**, 227 (1961); **131**, 355 (1963).

[5] P. Ring and P. Schuck, "Nuclear Many Body Problem," Springer-Verlag, New York/Berlin, 1980.

[6] M. Brack, C. Guet and H.-B. Hakansson, Phys. Rep. **123**, 275 (1985).

[7] K. A. Brueckner, J. H. Chirico and H. W. Meldner, Phys. Rev. **C 4**, 732 (1971).

[8] A. K. Dutta, J.-P. Arcoragi, J. M. Pearson, R. Behrman and F. Tondeur, Nucl. Phys. **A 458**, 77 (1986).

[9] F. Tondeur, A. K. Dutta, J. M. Pearson and R. Behrman, Nucl. Phys. **A 470**, 93 (1987).

[10] J. M. Pearson, Y. Aboussir, A. K. Dutta, R. C. Nayak, M. Farine and F. Tondeur, Nucl. Phys. **A 528**, 1 (1991).

[11] Y. Aboussir, J. M. Pearson, A. K. Dutta and F. Tondeur, *Nucl. Phys. A* **549**, 155 (1992).

[12] F. Garcias, M. Barranco, J. Nemeth and C. Ngô, *Phys. Lett. B* **206**, 177 (1988).

[13] F. Garcias, M. Barranco, J. Nemeth, C. Ngô and X. Viñas, *Nucl. Phys. A* **495**, 169 (1989).

[14] W. D. Myers and W. J. Swiatecki, *Ann. Phys. (N.Y.)* **204**, 401 (1990).

[15] W. D. Myers and W. J. Swiatecki, *Ann. Phys. (N.Y.)* **211**, 292 (1991).

[16] P. Möller, J. R. Nix, W. D. Myers and W. J. Swiatecki, "Nuclear Ground State Masses and Deformations," Los Alamos preprint LA-UR-93-3083, Aug. 16, 1993, to be published in the Atomic Data and Nuclear Data Tables.

[17] W.D. Myers and W. J. Swiatecki, *Nucl. Phys.* **81**, 1 (1966).

[18] R. W. Hasse and W. D. Myers, "Geometrical Relationships of Macroscopic Nuclear Physics," Springer-Verlag, New York/Berlin, 1988.

[19] W. D. Myers and W. J. Swiatecki, "The Nuclear Thomas-Fermi Model," Proc. XXIX, Zakopane School of Physics, 5–14 September 1994, Zakopane, Poland, to be published in Acta Physica Polonica.

[20] W. D. Myers, "Droplet Model of Atomic Nuclei," IFI/Plenum, New York, 1977.

[21] B. Friedman and V. R. Pandharipande, *Nucl. Phys. A* **361**, 502 (1981).
[22] H. de Vries, C. W. Jager and C. de Vries, *At. Data Nucl. Data Tables* **36**, 495 (1987).
[23] W. J. Swiatecki, Ph.D. Thesis, University of Birmingham, October 1949, unpublished.
[24] W. J. Swiatecki, *Physica Scripta* **28**, 349 (1983).
[25] W. D. Myers and W. J. Swiatecki, *Ann. Phys. (N.Y.)* **55**, 395 (1969).
[26] W. D. Myers and W. J. Swiatecki, *Ann. Phys. (N.Y.)* **84**, 186 (1974).
[27] C. O. Dorso, W. D. Myers and W. J. Swiatecki, *Nucl. Phys. A* **451**, 189 (1986).
[28] W. D. Myers and W. J. Swiatecki, *Nucl. Phys. A* **531**, 93 (1991).
[29] W. Stocker, J. Bartel, J. R. Nix and A. J. Sierk, *Nucl. Phys. A* **489**, 252 (1988).
[30] M. Durand, P. Schuck and X. Viñas, *Zeit. f. Physik A* **346**, 87 (1993).

LAWRENCE BERKELEY LABORATORY
UNIVERSITY OF CALIFORNIA
TECHNICAL INFORMATION DEPARTMENT
BERKELEY, CALIFORNIA 94720